A Novel Peroxisome Proliferator-activated Receptor (PPAR)α Agonist and PPARγ Antagonist, Z-551, Ameliorates High-fat Diet-induced Obesity and Metabolic Disorders in Mice[*]

Yoshihiro Shiomi[‡1], Toshimasa Yamauchi[‡§], Masato Iwabu[‡], Miki Okada-Iwabu[‡], Ryo Nakayama[‡], Yuki Orikawa[¶], Yoshichika Yoshioka[‖], Koichiro Tanaka[¶2], Kohjiro Ueki[‡], and Takashi Kadowaki[‡3]

From the Departments of [‡]Diabetes and Metabolic Diseases, Graduate School of Medicine and [§]Integrated Molecular Science on Metabolic Diseases, 22nd Century Medical and Research Center, The University of Tokyo, Tokyo 113-8655, Japan, [¶]Central Research Laboratories, Zeria Pharmaceutical Co., Ltd., Saitama 360-0111, Japan, and the [‖]Laboratory of Biofunctional Imaging, Immunology Frontier Research Center, Osaka University, Osaka 565-0871, Japan

Background: Obesity is one of the principal causes of metabolic syndrome.
Results: A novel PPARα agonist/γ antagonist, Z-551, ameliorates obesity, insulin resistance, and impairment of glucose and lipid metabolisms in mice.
Conclusion: Z-551 might be clinically useful for preventing or treating obesity and obesity-related metabolic disorders.
Significance: A novel combination of PPARα agonist/γ antagonist is effective to improve obesity and obesity-related metabolic disorders.

A novel peroxisome proliferator-activated receptor (PPAR) modulator, Z-551, having both PPARα agonistic and PPARγ antagonistic activities, has been developed for the treatment of obesity and obesity-related metabolic disorders. We examined the effects of Z-551 on obesity and the metabolic disorders in wild-type mice on the high-fat diet (HFD). In mice on the HFD, Z-551 significantly suppressed body weight gain and ameliorated insulin resistance and abnormal glucose and lipid metabolisms. Z-551 inhibited visceral fat mass gain and adipocyte hypertrophy, and reduced molecules involved in fatty acid uptake and synthesis, macrophage infiltration, and inflammation in adipose tissue. Z-551 increased molecules involved in fatty acid combustion, while reduced molecules associated with gluconeogenesis in the liver. Furthermore, Z-551 significantly reduced fasting plasma levels of glucose, triglyceride, free fatty acid, insulin, and leptin. To elucidate the significance of the PPAR combination, we examined the effects of Z-551 in PPARα-deficient mice and those of a synthetic PPARγ antagonist in wild-type mice on the HFD. Both drugs showed similar, but weaker effects on body weight, insulin resistance and specific events provoked in adipose tissue compared with those of Z-551 as described above, except for lack of effects on fasting plasma triglyceride and free fatty acid levels. These findings suggest that Z-551 ameliorates HFD-induced obesity, insulin resistance, and impairment of glucose and lipid metabolisms by PPARα agonistic and PPARγ antagonistic activities, and therefore, might be clinically useful for preventing or treating obesity
and obesity-related metabolic disorders such as insulin resistance, type 2 diabetes, and dyslipidemia.

Obesity is one of the principal causes of metabolic syndrome, and has currently become a serious social problem (1, 2). Excess energy due to overeating or a lack of physical activity causes increased accumulation of subcutaneous and visceral fat, resulting in adipocyte hypertrophy, macrophage infiltration into the adipose tissue, and abnormal adipokine productions (3). Free fatty acids (FFA)[4] and adipokines including monocyte chemoattractant protein-1 (MCP-1) and TNF-α overproduced by hypertrophic adipocytes infiltrated with macrophages especially in visceral fat are known to provoke and induce systemic chronic inflammation, insulin resistance, and impairment of glucose and lipid metabolisms by inhibiting insulin-signaling pathway in target organs such as the liver and skeletal muscle (4–6). Thus, visceral fat obesity has been elucidated to be closely related to the onset of obesity-related metabolic disorders such as insulin resistance, type 2 diabetes, dyslipidemia, and fatty liver diseases. Accordingly, drugs that can counteract obesity by inhibiting visceral fat accumulation, may provide an effective treatment of insulin resistance and obesity-related metabolic disorders. Drugs that may increase the expenditure of excess energy stored as triglyceride (TG) are also desirable.

PPARs are ligand-activated transcription factors and belong to a nuclear receptor superfamily, which consists of three subtypes (α, γ, and δ) in mammals (7, 8). PPARα and PPARγ have been noticed as therapeutic targets for dyslipidemia and type 2 diabetes, respectively. PPARα is mainly expressed in the liver, and plays wide-ranging roles in lipid metabolism, energy homeo-

stasis, and inflammation (9, 10). Fibrates, PPARα agonists, and drugs for dyslipidemia promote peroxisomal and mitochondrial β-oxidation, and inhibit fatty acid synthesis in the liver due to activation of PPARα, resulting in amelioration of insulin resistance owing to decreased ectopic fat accumulation in peripheral tissues (11–15). On the other hand, PPARγ has two isoforms, PPARγ1 and PPARγ2 formed by selective splicing. PPARγ1 is expressed at low levels in many tissues, whereas PPARγ2 is specifically expressed in the adipose tissue and functions as a master regulator in adipocyte differentiation and glucose metabolism (16). Thiazolidinediones (TZDs), PPARγ agonists, and drugs for type 2 diabetes promote loss of hypertrophic adipocytes by apoptosis and differentiation of preadipocytes into normal adipocytes, thereby preventing adipocyte hypertrophy and ameliorating insulin resistance (17, 18), whereas these drugs cause weight gain. In contrast, we have reported that heterozygous PPARγ-deficient (PPARγ$^{+/-}$) mice are resistant to high-fat diet (HFD)-induced obesity, adipocyte hypertrophy, and insulin resistance (18–20). Consistent with these observations, the Pro12Ala polymorphism in the human *PPARγ2* gene resulting in partial reduction of PPARγ transcriptional activity has been shown to be associated with reduced weight gain and improved insulin sensitivity (21, 22). Inhibition of PPARγ activity by the retinoid X receptor (RXR) antagonist (23) or PPARγ antagonists (24, 25) has been reported to ameliorate HFD-induced obesity and insulin resistance by inhibiting fat accumulation in adipocytes. These findings suggest that inhibiting the onset and progression of obesity is essential for prevention and treatment of obesity-related metabolic disorders. These results indicate that PPARγ antagonists could be potential drugs to prevent and treat obesity and obesity-related metabolic disorders and may be even more superior to PPARγ agonists in terms of suppression of fat formation and improvement of glucose metabolism (26). Taken together, it is desirable to utilize a PPAR modulator having both PPARα agonistic and PPARγ antagonistic activities as an effective treatment of diet-induced obesity, insulin resistance, and impairment of glucose and lipid metabolisms by suppressing visceral fat accumulation and increasing energy expenditure in our concept of drug discovery.

Based on these backgrounds, to develop a drug with a novel mechanism of action for the prevention or treatment of obesity and obesity-related metabolic disorders, we have designed a novel PPAR modulator, Z-551, which has both PPARα agonistic and PPARγ antagonistic activities.

In the present study, we examined the preventive and therapeutic effects of Z-551 on obesity and obesity-related metabolic disorders in two different animal models, wild-type (WT) mice and wild-type diet-induced obese (WT DIO) mice on the HFD. To elucidate the contribution of PPARγ antagonistic activities of Z-551 and the significance of the PPAR combination, we examined the effects of Z-551 in PPARα-deficient mice and those of a selective PPARγ antagonist, CZD-2, in WT mice on HFD. Finally, we will discuss the potential of Z-551 as a drug for preventing or treating obesity and obesity-related metabolic disorders such as insulin resistance, type 2 diabetes, dyslipidemia, and fatty liver diseases.

Experimental Procedures

Chemicals—A PPARα agonist and PPARγ antagonist, Z-551 (Monosodium 2-{9-[(3-methoxy-4-{[5-methyl-2-phenyl(1,3-oxazol-4-yl)]methoxy}phenyl)methyl]carbazol-4-yloxy}-2-methylpropanoate, WO/2006046779), a PPARγ antagonist, CZD-2 (Carbazol derivative-2, Monosodium (2R)-2-{9-[(3-methoxy-4-{[5-methyl-2-phenyl(1,3-oxazol-4-yl)]methoxy}phenyl)methyl]carbazol-4-yloxy}butanoate, WO/2006046779), and GW501516 (PPARδ agonist) were synthesized at Central Research Laboratories of Zeria Pharmaceutical Co., Ltd. (Saitama, Japan). Wy-14643 (PPARα agonist) and rosiglitazone (PPARγ agonist) were purchased from Sigma-Aldrich, and Alexis Biochemicals (Lausanne, Switzerland), respectively.

Cell Culture—CV-1 cells were purchased from American Type Culture Collection (ATCC, Manassas, VA). CV-1 cells were cultured in DMEM (Invitrogen, Carlsbad, CA) supplemented with 10% charcoal-treated FBS (Dainippon Pharmaceutical Co., Ltd., Osaka, Japan) and 1% Antibiotic-Antimycotic solution (Invitrogen) at 37 °C in 5% CO_2.

Luciferase Reporter Assay—Luciferase reporter plasmid (pPPRE3-TK-Luc) was prepared by insertion of the thymidine kinase (TK) promoter region and three repeats of the PPAR response elements (PPRE) region (PPRE×3) into the pGL3 basic vector (Promega, Madison, WI), which is a luciferase expression vector. Each expression vector was constructed by individually inserting the full-length PPARα, PPARγ2, PPARδ, or RXRα gene from mouse or human into the pCI-neo mammalian expression vector (Promega). CV-1 cells (2×10^4 cells/well) were subcultured in 96-well plates overnight and the cells were transiently co-transfected with pPPRE3-TK-Luc, *Renilla* luciferase reporter plasmid (phRL-TK Vector, Promega), RXRα, and PPAR (PPARα, -γ2, or -δ) expression plasmids using Lipofectamine (Invitrogen). After 5 h, the cells were exposed to the test compounds, Wy-14643, rosiglitazone, GW501516, or 0.2% DMSO (vehicle) for 24 h. Luciferase assay was performed using a Dual Luciferase Assay System (Promega) and luciferase activities were measured using a multiplate reader (ARVO 1420, Perkin-Elmer, Shelton, CT). Luciferase activities were normalized by *Renilla* luciferase activities as an internal standard.

Animals—Male C57BL/6J mice (WT mice) were purchased from Charles River Japan (Yokohama, Japan). 129S4/SvJae-PparatmiGonz/J mice (PPARα-deficient mice) were purchased from Jackson Laboratories (Bar Harbor, ME) and the male PPARα-deficient mice were obtained by crossbreeding. Mice were group-housed on a 12-h light/dark cycle in an animal room maintained at 23 ± 3 °C, and fed *ad libitum* either a normal diet (ND) (CE-2, CLEA Japan, Tokyo, Japan) or a HFD (32.0% safflower, 33.1% casein, 0.5% DL-methionine, 17.6% sucrose, 1.4% vitamin mixture, 9.8% mineral mixture, and 5.6% cellulose powder) (27). Cumulative food intake was measured every 2 weeks over an 8-week period in an individual group and the food intake was expressed as an amount of food consumed (g/day/mouse). All the experiments in the present study were conducted on male littermates. The animal care and experimental procedures were approved by the Animal Care Committee of the University of Tokyo.

Drug Administration—1) To examine the preventive effects of Z-551 or CZD-2 in C57BL/6J mice (WT mice) and PPARα-deficient mice on the HFD (Figs. 2, 3, 6, 7, and 8), 4-week-old male mice were acclimatized to the HFD for 1 week followed by administration of Z-551 or CZD-2 for 9 to 16 weeks. 2) To examine the therapeutic effects of Z-551 in wild-type diet-induced obese (WT DIO) C57BL6/J mice (Figs. 4 and 5), 4-week-old male mice were given the HFD for 10 to 14 weeks and then administered Z-551 for 8 to 16 weeks. Z-551 and CZD-2 were given as a 0.1% (w/w) food admixture. In all experiments, based on the two factors of body weight and fasting plasma glucose level, the mice were assigned to a control group and a group of drug-treatment before administration of the drugs.

Glucose Homeostasis—The oral glucose tolerance test (OGTT) and insulin tolerance test (ITT) were performed by the methods described previously (28) with slight modifications regarding the amounts of glucose and insulin administered, and fasting periods as described in the figure legends. The pyruvate challenge test was conducted as described previously (29).

Assays for Blood and Tissue Samples—Plasma glucose and insulin levels were determined using a GluTest ProR (Sanwa Kagaku Research, Nagoya, Japan), and an Insulin ELISA Kit (Shibayagi, Gunma, Japan), respectively. Plasma TG and FFA levels were measured using a Triglyceride E-Test Wako and a NEFA C-Test Wako (Wako Pure Chemical Industries, Osaka, Japan), respectively. Plasma leptin levels were determined using a Leptin ELISA Kit (Morinaga Institute of Biological Science, Yokohama, Japan). Tissue TG in the liver and skeletal muscle was extracted with a hexane/isopropanol mixture (3:2, v/v) from the tissue homogenate, and dissolved in dioxane after evaporation at room temperature, followed by measurement using a Triglyceride E-Test Wako. The thiobarbituric acid reactive substance (TBARS) levels in the liver were determined using a TBARS Assay Kit (ZeptoMetrix Corporation, Buffalo, NY) according to the manufacturer's instructions.

Rectal Temperature—Rectal temperature was measured by inserting a digital thermistor thermometer (KN-91, Natsume Seisakusho, Tokyo, Japan) into the mouse rectum.

Oxygen Consumption—Oxygen consumption was measured every 1 h for 24 h in WT mice on the HFD using an O_2/CO_2 metabolism measurement device (Oxymax system; model 7540, Columbus Instruments, Columbus, OH). After Z-551 treatment for 3 weeks, each mouse was placed in a sealed chamber with an air flow rate of 600 ml/min at room temperature. The amount of oxygen consumed was normalized by body weight of each mouse and expressed as liter/kg/h.

Histological Analysis—The isolated epididymal white adipose tissue (WAT) and liver were fixed in 10% formaldehyde/PBS, and maintained at 4 °C until use. The fixed tissues were dehydrated and processed for paraffin embedding, and 10-μm sections were cut and mounted on silanized slides, followed by staining with hematoxylin and eosin (HE) (18).

Measurement of Adipocyte Size—The adipocyte size was measured by the method described previously (18) with slight modifications. In brief, the epididymal WAT was routinely processed for paraffin embedding, and 10-μm sections were cut and mounted on silanized slides, followed by staining with HE. The individual adipocyte area was manually traced and the adipocyte size was analyzed with Image J software (NIH, Bethesda, MD). The white adipocyte size was measured in 200 cells/mouse in each group.

Real-time Quantitative RT-PCR—Real-time quantitative RT-PCR was performed by the method described previously (30, 31). Total RNA was prepared from the epididymal WAT and liver using TRIzol (Invitrogen) according to the manufacturer's instructions. After purification, total RNA was converted into first-strand cDNA. The first-strand cDNA obtained was subjected to real-time quantitative PCR with TaqMan Gene Expression Master Mix (Applied Biosystems, Foster City, CA) and TaqMan Gene Expression Assays (Applied Biosystems) containing a set of TaqMan probe and PCR primers for each gene using an ABI PRISM 7900 Sequence Detection System (Applied Biosystems). The TaqMan probes were used for mouse acyl-CoA oxidase 1 (ACOX1 encoded by *Acox1*), Mm01184029_m1; CD206 (*Mrc1*), Mm00485148_m1; CD36 (*Cd36*), Mm 01135198_m1; CD68 (*Cd68*), Mm00839636_g1; F4/80 (*Emr1*), Mm00802530_m1; fatty acid synthase (FAS, *Fasn*), Mm01253292_m1; IL-1β (*Il1b*), Mm00434228_m1; leptin (*Lep*), Mm 00434759_m1; lipoprotein lipase (LPL, *Lpl*), Mm00434764_m1; macrophage-1 antigen (Mac-1, *Itgam*), Mm00434455_m1; monocyte chemoattractant protein-1 (MCP-1, *Ccl2*), Mm 00441242_m1; phosphoenolpyruvate carboxykinase (PEPCK, *Pck1*), Mm 00447183_m1; peroxisome proliferator-activated receptor γ coactivator 1α (PGC1α, *Ppargc1a*), Mm 01344232_g1; sterol regulatory element-binding protein-1c (SREBP-1c, *Srebf1*), Mm 00550338_m1; TNF-α (*Tnf*), Mm00443260_g1; Toll-like receptor 4 (TLR4, *Tlr4*), Mm 00494069_m1; uncoupling protein 1 (UCP1, *Ucp1*), Mm00445273_m1; uncoupling protein 2 (UCP2, *Ucp2*), Mm00495907_g1; 36B4 (*Rplp0*), Mm00725448_s1. The primers and the probe for mouse cyclophilin A (*Ppia*) were as follows: the forward primer was 5′-ggtcctggcatcttgtccat-3′, the reverse primer was 5′-cagtcttggcagtgcagataaaa-3′, and the probe was 5′-ctggaccaaacacaaacggttccca-3′ (31). The relative amount of each transcript was normalized to the amount of *Rplp0* or *Ppia* transcripts as internal standards.

Akt Phosphorylation—Mice were anesthetized after 6-h fasting, and insulin (0.5 unit/kg of body weight) (Humulin R, Eli Lilly, Indianapolis, IN) or saline (vehicle) was injected into the inferior vena cava, followed by isolating the liver and skeletal muscle 5 min later. Western blot analysis was carried out as described previously (32). The Akt phosphorylation was analyzed using rabbit anti-mouse phospho-Akt (Ser-473) antibody (Cell Signaling Technology Inc., Beverly, MA) and rabbit anti-mouse Akt antibody (Santa Cruz Biotechnology, Santa Cruz, CA). The insulin-stimulated Akt phosphorylation was expressed as a ratio of phosphorylated Akt to Akt (pAkt/Akt).

Peripheral Quantitative Computed Tomography (pQCT)—The right femur was removed from each mouse. The isolated femur was fixed in 80% alcohol, and maintained at 4 °C until use. pQCT was performed using an XCT Research SA Plus (Stratec Medizintechnik GmbH, Pforzheim, Germany). Total and trabecular bone mineral densities in the proximal femur of mice were measured by the method described previously (33).
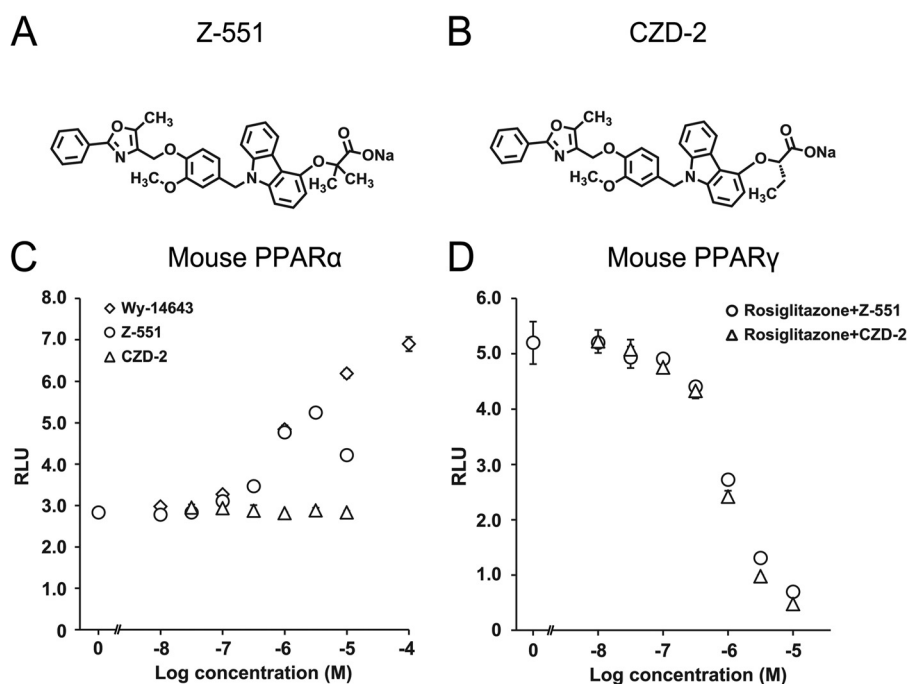
FIGURE 1. **Z-551 is a novel PPAR modulator having both PPARα agonistic and PPARγ antagonistic activities.** *A* and *B*, chemical structures of Z-551 (*A*) and CZD-2 (*B*). *C* and *D*, effects of Z-551 and CZD-2 on transcriptional activities for mouse PPARα (*C*) and PPARγ (*D*). All results are expressed as mean ± S.E. (*n* = 4). EC_{50} values for PPARα are calculated on the assumption that the maximum transcriptional activity induced by Wy-14643 is 100%. IC_{50} values for PPARγ are calculated on the assumption that the transcriptional activity induced by 100 nm rosiglitazone is 100%.

Magnetic Resonance Imaging (MRI) and Magnetic Resonance Spectroscopy (MRS)—An 11.7 T MRI scanner (AVANCE-II 500 WB, Bruker BioSpin, Ettlingen, Germany) was used to acquire *ex vivo* femur bone images and spectra. A T2-weighted imaging sequence (RARE) with the following parameters was used: field of view, 12.8 mm×12.8 mm; matrix size, 512 × 512; slice thickness, 0.1 mm; repetition time, 5,000 ms; echo time, 7.8 ms; average, 40; scan time, 14 h. MR spectra were obtained by a point resolved spectroscopy sequence (PRESS) with the following parameters: spectral width, 6,000 Hz; data size, 8,196 points; volume of interest, 0.7 mm cubic; repetition time, 4,000 ms; echo time, 20 ms; average, 64; scan time, 4.3 min (34).

Statistical Analysis—All the results were expressed as means ± S.E. Difference between two groups was assessed using Student's *t* test. Data involving more than two groups were assessed by analysis of variance statistical (ANOVA) and Dunnett's test. $p < 0.05$ was considered statistically significant.

Results

Z-551 Is a Novel PPAR Modulator Having Both PPARα Agonistic and PPARγ Antagonistic Activities—Agonistic and antagonistic activities of Z-551 (structure shown in Fig. 1*A*) for each PPAR were quantitatively determined by the luciferase reporter assay. Z-551 indicated partial agonistic activities for mouse and human PPARα with half-maximal effective concentrations (EC_{50} values) of 539 nm and 1.22 μm, respectively (Fig. 1*C*). The maximal agonistic activities for both species were ~60% of that of PPARα full agonist, Wy-14643. In addition, Z-551 exhibited antagonistic activities for mouse and human PPARγ with half-maximal inhibitory concentrations (IC_{50} values) of 956 nm and 481 nm, respectively (Fig. 1*D*), obtained with PPARγ full agonist, rosiglitazone. These results indicate no significant differ-

ences in the PPARα agonistic or PPARγ antagonistic activity of Z-551 between mouse and human. In contrast, Z-551 indicated neither agonistic nor antagonistic activity for mouse and human PPARδ. These results indicate that Z-551 is a novel dual PPAR modulator, which has both PPARα partial agonistic and PPARγ antagonistic activities.

Z-551 Has Preventive Effects on HFD-induced Obesity and Obesity-related Metabolic Disorders in WT Mice on the HFD—To elucidate preventive effects of Z-551 on HFD-induced obesity and obesity-related metabolic disorders, we examined the effects using WT mice on the HFD. Z-551 significantly suppressed an increase in body weight without any effect on food intake, and weight of the visceral fat tissue and epididymal WAT, compared with the mice on the HFD alone (control) (Fig. 2, *A–C*). In the epididymal WAT, histological analysis showed that HFD-induced hypertrophy of adipocytes was suppressed by administration of Z-551 (Fig. 2*D*). Gene expression analysis in the epididymal WAT demonstrated that Z-551 significantly inhibited gene expressions involved in fatty acid uptake (*Lpl* and *Cd36*), fatty acid synthesis (*Fasn*), energy metabolism (*Lep*), macrophage recruitment (*Ccl2*), and cell surface markers of macrophage (*Emr1*) (Fig. 2*E*). Furthermore, Z-551 significantly reduced plasma leptin levels as well as mRNA levels (Fig. 2*F*). These findings indicate that Z-551 has anti-obesity effects and inhibits adipocyte hypertrophy and macrophage infiltration in adipose tissue. In the liver, the histological analysis showed that Z-551 suppressed the formation of large lipid droplets, compared with the control (Fig. 2*G*). Z-551 also significantly increased liver weight (Fig. 2*H*). The gene expression analysis in the liver demonstrated that Z-551 significantly increased gene expressions involved in fatty acid uptake (*Lpl* and *Cd36*), fatty
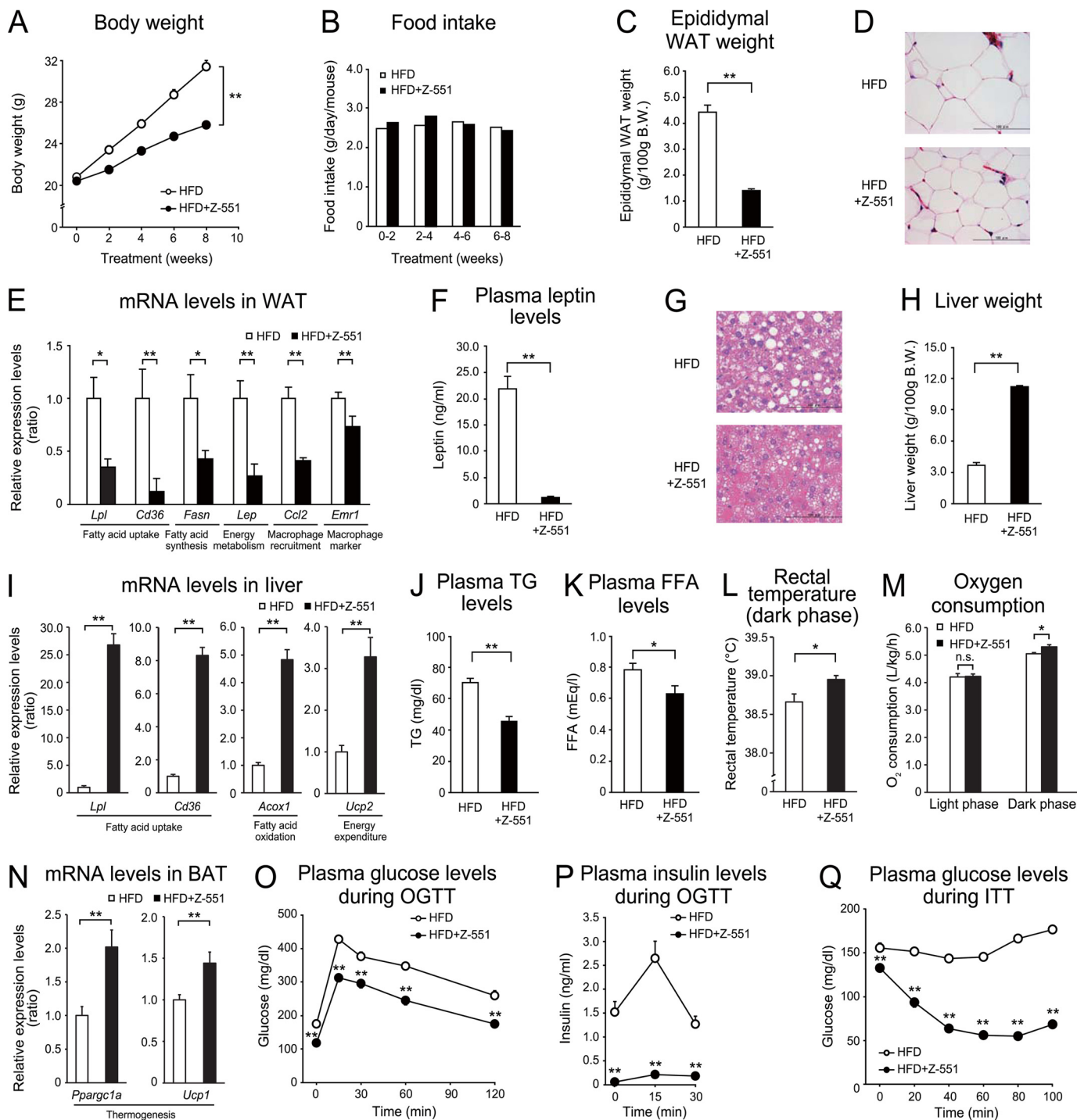
FIGURE 2. **Z-551 indicates preventive effects on diet-induced obesity and metabolic disorders in WT mice.** 4-week-old male WT mice were acclimatized to the HFD for 1 week followed by administration of Z-551 for 9 weeks. *A–C*, changes in body weight (*A*), food intake (*B*), and epididymal WAT weight (*C*) in WT mice on the HFD (*white*) or HFD+Z-551 (*black*). *D*, morphology of epididymal WAT. Scale bars indicate 100 μm. *E*, mRNA expression levels in epididymal WAT. *F*, plasma leptin Week 8 after Z-551 administration. *G*, morphology of liver. Scale bars indicate 100 μm. *H*, liver weight, *I*, mRNA expression levels in the liver. *J* and *K*, plasma TG (*J*) and FFA (*K*) Week 4 after Z-551 administration. *L*, rectal temperature. Rectal temperature was measured during the dark phase Week 9 after Z-551 administration. *M*, oxygen consumption. Oxygen consumption was measured Week 3 after Z-551 administration. *N*, mRNA expression levels in BAT. *O* and *P*, plasma glucose (*O*) and insulin (*P*) in the OGTT Week 5 after Z-551 administration. *Q*, plasma glucose in the ITT Week 8 after Z-551 administration. In the OGTT, glucose (1.0 g/kg body weight (BW)) was orally administered after 6-h fasting. In the ITT, insulin (0.75 unit/kg BW) was intraperitoneally injected. Blood samples were obtained at the indicated times. All results are expressed as mean ± S.E. (n = 7–10). *, $p < 0.05$; **, $p < 0.01$; *n.s.*, not significant.

acid oxidation (*Acox1*), and energy expenditure (*Ucp2*) (Fig. 2*I*). These findings indicate that Z-551 enhances fatty acid combustion including fatty acid uptake, fatty acid oxidation, and energy expenditure in the liver. Consistent with these results, plasma

TG and FFA levels were significantly reduced by administration of Z-551 (Fig. 2, *J* and *K*). To determine whether the basal metabolism is altered by administration of Z-551, we measured the rectal temperature and oxygen consumption. Z-551 signif-
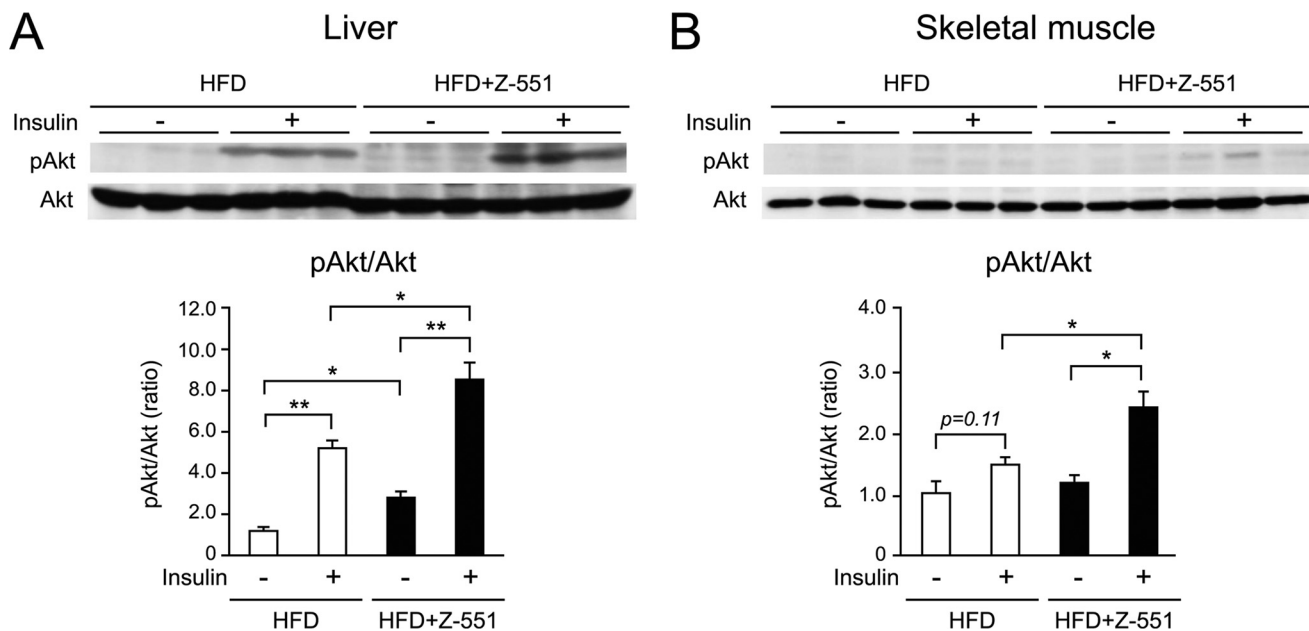
FIGURE 3. **Z-551 improves insulin sensitivity in the liver and skeletal muscle of WT mice.** 4-week-old male WT mice were acclimatized to the HFD for 1 week followed by administration of Z-551 for 15 weeks. *A* and *B*, insulin-stimulated Akt (Ser-473) phosphorylation in the liver (*A*) and skeletal muscle (*B*) of WT mice on the HFD (*white*) or HFD+Z-551 (*black*). The phosphorylation and amount of Akt were analyzed by Western blot (*upper panel*) and the ratio of phosphorylated Akt to Akt (pAkt/Akt) is calculated (*lower panel*). All results are expressed as mean ± S.E. (*n* = 3). *, $p < 0.05$; **, $p < 0.01$.

icantly raised the rectal temperature and oxygen consumption during the active period in the dark phase in WT mice on the HFD (Fig. 2, *L* and *M*). Z-551 did not change the oxygen consumption per mice in the dark phase despite showing significant decrease of body weight compared with the control, indicating that Z-551 significantly increased oxygen consumption per body weight (Fig. 2*M*). These findings suggest that oxygen consumption is one of causes of anti-obesity effects by Z-551 administration. Furthermore, Z-551 significantly increased the expression levels of brown adipose tissue (BAT) markers of thermogenesis such as *Ppargc1a* and *Ucp1*, suggesting that Z-551 activated the thermogenesis in BAT of the mice (Fig. 2*N*). On the other hand, Z-551 had no effect on the cumulative fecal weight and lipids excreted in feces for 2 weeks after starting Z-551 administration (data not shown). The OGTT and ITT were performed to elucidate the effects of Z-551 on insulin resistance in WT mice on the HFD. The OGTT indicated that Z-551 significantly decreased plasma glucose and insulin levels after glucose administration compared with the control, and attenuated the glucose intolerance (Fig. 2, *O* and *P*). The ITT indicated that Z-551 significantly decreased plasma glucose levels after insulin injection, and improved decreased insulin sensitivity induced by the HFD (Fig. 2*Q*).

The Western blot analysis showed that Z-551 significantly increased insulin-stimulated Akt (Ser-473) phosphorylation in the liver, skeletal muscle (Fig. 3, *A* and *B*), and epididymal WAT (data not shown), suggesting that Z-551 enhances insulin sensitivity. Z-551 significantly reduced increased fasting plasma glucose and insulin levels, which were shown at time zero in the OGTT (Fig. 2, *O* and *P*). These results indicate that Z-551 significantly improved hyperglycemia and hyperinsulinemia in WT mice on the HFD. Taken together, these findings suggest that Z-551 has preventive effects on HFD-induced obesity and obesity-related metabolic disorders due to ameliorating HFD-

induced obesity, insulin resistance, and abnormal glucose and lipid metabolisms.

Z-551 Has Therapeutic Effects on HFD-induced Obesity and Obesity-related Metabolic Disorders in WT DIO Mice—To elucidate the therapeutic effects of Z-551 on HFD-induced obesity and obesity-related metabolic disorders, we examined the effects using WT DIO mice. The results demonstrate that the therapeutic effects of Z-551 were essentially comparable to the preventive effects in WT mice on the HFD as described above (Fig. 2). Z-551 significantly suppressed increased body weight without changing food intake (data not shown), increased epididymal WAT weight and adipocyte hypertrophy induced by the HFD compared with the control (Fig. 4, *A–C*, Fig. 5, *A–D*). In the epididymal WAT, Z-551 significantly inhibited gene expressions involved in fatty acid uptake (*Lpl* and *Cd36*) and energy metabolism (*Lep*) (Fig. 5*E*). We examined the effects of Z-551 on macrophage infiltration and inflammation in the adipose tissue in detail. Z-551 significantly inhibited the expressions of common macrophage markers (*Emr1*, *Cd68*, and *Itgam*), classically activated (M1) macrophage markers (*Ccl2* and *Tlr4*), and M1 macrophage/inflammation markers (*Tnf* and *Il1b*), whereas Z-551 had no effect on the expression of an alternatively activated (M2) macrophage marker (*Mrc1*) (Figs. 4*D* and 5*E*). Z-551 also significantly reduced plasma leptin levels as well as mRNA levels (Fig. 4*E*). These findings indicate that Z-551 not only has anti-obesity effects and inhibits adipocyte hypertrophy and macrophage infiltration in the adipose tissue similar to the preventive effects of Z-551 as described above, but also suppresses inflammation in adipose tissue. In the liver, similarly, Z-551 suppressed the formation of large lipid droplets in the liver (Fig. 4*F*), whereas Z-551 significantly increased liver weight compared with the control (Fig. 4*G*). The gene expression analysis in the liver also showed similar profiles involved in fatty acid uptake (*Lpl* and *Cd36*), fatty
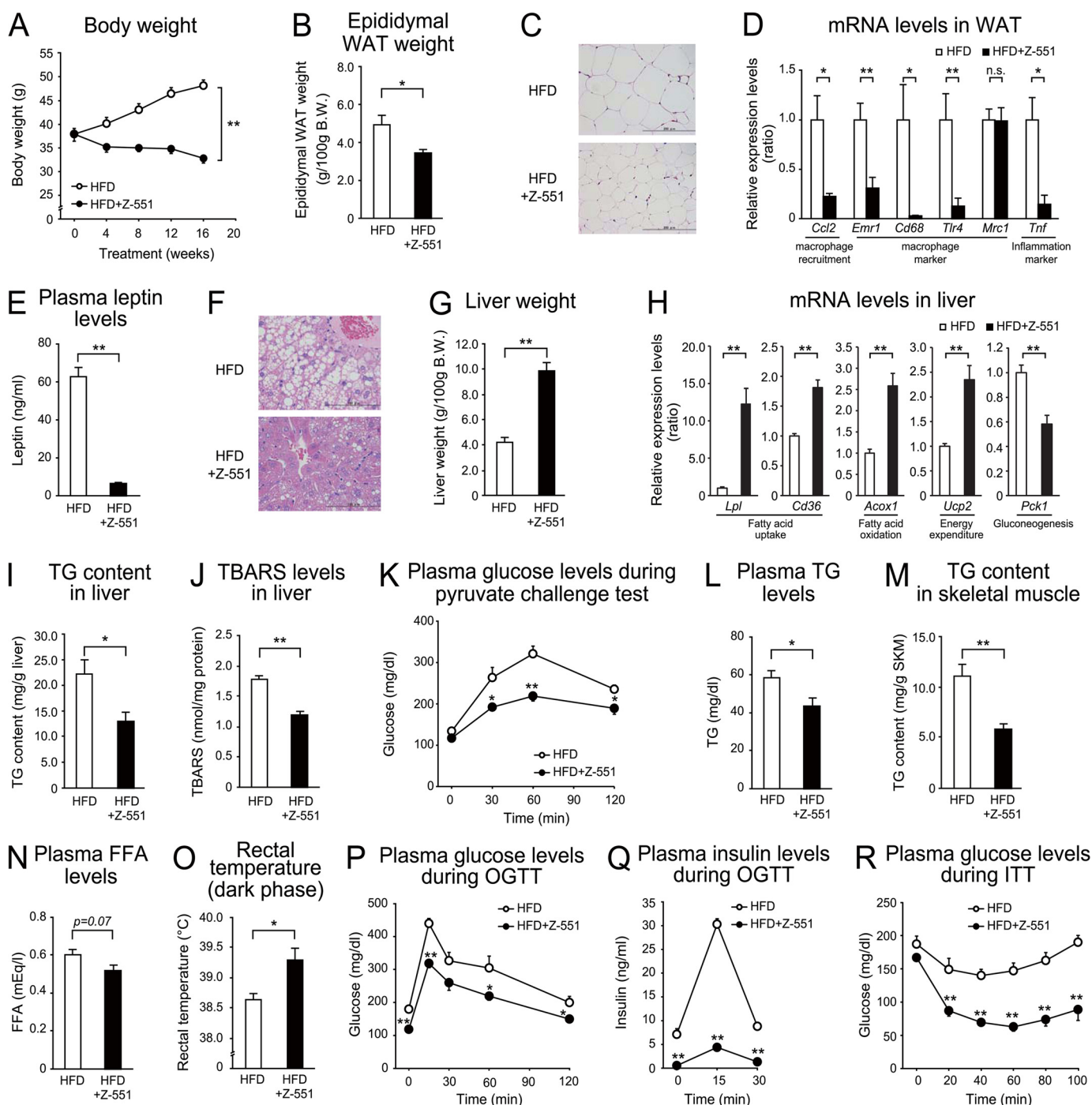
FIGURE 4. **Z-551 indicates therapeutic effects on diet-induced obesity and metabolic disorders in WT DIO mice-Experiment 1.** 4-week-old male WT mice were given the HFD for 14 weeks followed by administration of Z-551 for 16 weeks. *A* and *B*, changes in body weight (*A*), and epididymal WAT weight (*B*) in WT DIO mice on the HFD (*white*) or HFD+Z-551 (*black*). *C*, morphology of epididymal WAT. Scale bars indicate 200 μm. *D*, mRNA expression levels of in epididymal WAT. *E*, plasma leptin week 12 after Z-551 administration. *F*, morphology of the liver. Scale bars indicate 100 μm. *G*, liver weight. *H*, mRNA expression levels in the liver. *I* and *J*, TG content (*I*) and TBARS levels (*J*) in the liver. *K*, plasma glucose in the pyruvate challenge test Week 9 after Z-551 administration. In the pyruvate challenge test, sodium pyruvate (1.5 g/kg BW) was intraperitoneally injected after 6-h fasting and blood samples were obtained at the indicated times. *L* and *N*, plasma TG (*L*) and FFA (*N*) Week 13 after Z-551 administration. *M*, TG content in skeletal muscle. *O*, rectal temperature. Rectal temperature was measured during the dark phase Week 15 after Z-551 administration. *P* and *Q*, plasma glucose Week 7 after Z-551 administration. In the OGTT, glucose (1.5 g/kg BW) was orally administered after 6-h fasting. In the ITT, insulin (0.5 unit/kg BW) was intraperitoneally injected. Blood samples were obtained at the indicated times. All results are expressed as mean ± S.E. ($n = 6$). *, $p < 0.05$; **, $p < 0.01$; *n.s.*, not significant.

acid oxidation (*Acox1*), and energy expenditure (*Ucp2*) (Fig. 4*H*). We examined whether Z-551 had effects on TG content, oxidative stress, and gluconeogenesis in the liver. Z-551 significantly decreased concentrations of hepatic TG, and TBARS which is an indicator of lipid peroxidation (Fig. 4, *I* and *J*). Z-551 significantly inhibited gene expression of *Pck1* involved in gluconeogenesis in the liver and decreased plasma glucose levels in the pyruvate challenge test, which evaluates gluconeogenesis
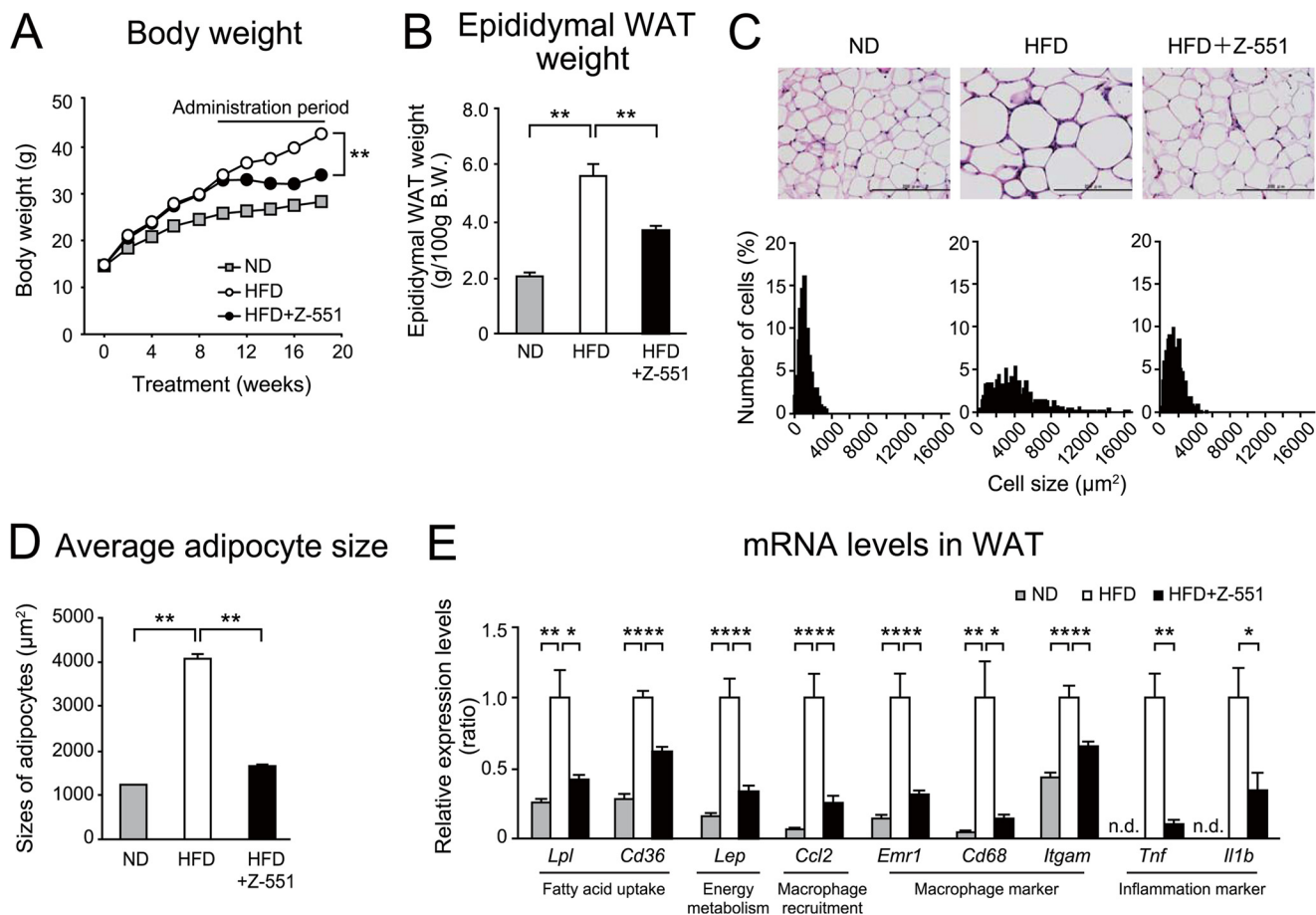
FIGURE 5. **Z-551 indicates therapeutic effects on diet-induced obesity and metabolic disorders in WT DIO mice-Experiment 2.** 4-week-old WT mice were given the HFD for 10 weeks and then administered Z-551 for 8 weeks. *A* and *B*, changes in body weight (*A*), and epididymal WAT weight (*B*) in WT mice on the ND (*gray*), and WT DIO mice on the HFD (*white*) or HFD+Z-551 (*black*). *C* and *D*, morphology of epididymal WAT (*upper panel*) and histogram of adipocyte size from epididymal WAT (*lower panel*) (*C*), and average size of adipocytes from epididymal WAT (*D*). Scale bars indicate 200 μm. *E*, mRNA expression levels in epididymal WAT. All results are expressed as mean ± S.E. ($n = 8$–10). *, $p < 0.05$; **, $p < 0.01$ compared with the obese mice on the HFD; *n.d.*, not detected.

(Fig. 4, *H* and *K*). These results indicate that Z-551 enhances fatty acid combustion including fatty acid uptake and fatty acid oxidation, and inhibits oxidative stress and gluconeogenesis in the liver. Furthermore, Z-551 significantly reduced plasma TG levels and ectopic TG accumulation in the skeletal muscle, and tended to reduce plasma FFA compared with the control (Fig. 4, *L–N*). Z-551 significantly raised the rectal temperature during the active period in the dark phase in WT DIO mice (Fig. 4*O*). The OGTT and ITT indicated that Z-551 had effects (Fig. 4, *P–R*) similar to the preventive action in WT mice on the HFD as described above (Fig. 2) by ameliorating the glucose intolerance and improving the reduced insulin sensitivity induced by the HFD. Likewise, Z-551 significantly improved hyperglycemia and hyperinsulinemia in WT DIO mice as shown by fasting plasma glucose and insulin levels (Fig. 4, *P* and *Q*). Taken together, these findings suggest that Z-551 has therapeutic effects on HFD-induced obesity and obesity-related metabolic disorders by ameliorating HFD-induced obesity, insulin resistance, and abnormal glucose and lipid metabolisms as well as the preventive effects.

Both PPARα Agonistic and PPARγ Antagonistic Activities of Z-551 Are Required for Ameliorating HFD-induced Obesity and Obesity-related Metabolic Disorders—To elucidate the contribution of PPARγ antagonistic activities of Z-551 and the signif-

icance of the PPAR combination, we examined the preventive effects of Z-551 using PPARα-deficient mice and those of a selective PPARγ antagonist, CZD-2 using WT mice on the HFD.

(i) Effects of Z-551 in PPARα-deficient Mice on the HFD— Z-551 significantly increased the expression of PPARα target genes in the liver of WT mice (Fig. 2), whereas no effect of Z-551 was found in the liver of PPARα-deficient mice (data not shown). Z-551 was found to have similar but weaker preventive effects in PPARα-deficient mice on the HFD (Fig. 6) compared with those in WT mice on the HFD as described above (Fig. 2), though no effects on fasting plasma TG and FFA levels and liver weight were observed. Z-551 significantly suppressed increases in body weight and epididymal WAT weight, though to lower degrees than those in WT mice on the HFD (Fig. 2) without changing food intake (data not shown), whereas Z-551 tended to inhibit an increase in body weight compared with the control (Fig. 6, *A–C*). Z-551 also suppressed adipocyte hypertrophy in the epididymal WAT induced by the HFD (Fig. 6*D*). In the epididymal WAT, gene expressions involved in fatty acid uptake (*Lpl* and *Cd36*), fatty acid synthesis (*Srebf1* and *Fasn*), energy metabolism (*Lep*), macrophage recruitment (*Ccl2*), and cell surface markers of macrophage (*Cd68*) were inhib-
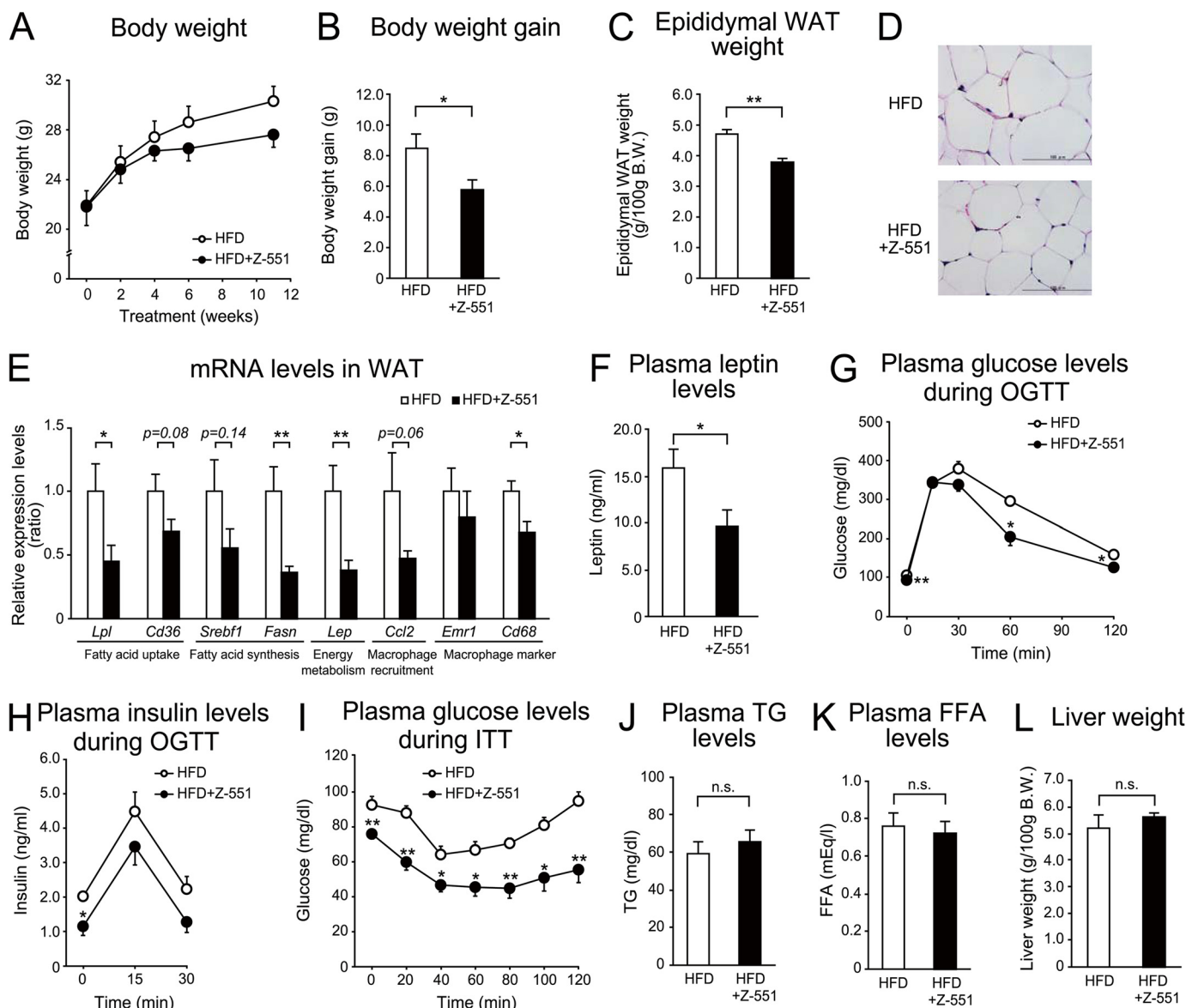
FIGURE 6. Z-551 indicates a part of the preventive effects on diet-induced obesity and metabolic disorders in PPARα-deficient mice. 4-week-old male PPARα-deficient mice were acclimated to the HFD for 1 week followed by administration of Z-551 for 11 weeks. *A–C*, changes in body weight (*A*), body weight gain (*B*), and epididymal WAT weight (*C*) in PPARα-deficient mice on the HFD (*white*) or HFD+Z-551 (*black*). *D*, morphology of epididymal WAT. Scale bars indicate 100 μm. *E*, mRNA expression levels in epididymal WAT of PPARα-deficient mice. *F*, plasma leptin Week 10 after Z-551 administration. *G* and *H*, plasma glucose (*G*) and insulin (*H*) in the OGTT Week 7 after Z-551 administration. *I*, plasma glucose in the ITT Week 8 after Z-551 administration. In the OGTT, glucose (2.0 g/kg BW) was orally administered after 6-h fasting. In the ITT, insulin (0.75 unit/kg BW) was intraperitoneally injected. Blood samples were obtained at the indicated times. *J* and *K*, plasma TG (*J*) and FFA (*K*) Week 10 after Z-551 administration. *L*, liver weight. All results are expressed as mean ± S.E. ($n = 5$–8). *, $p < 0.05$; **, $p < 0.01$; *n.s.*, not significant.

ited by administration of Z-551 (Fig. 6*E*). Z-551 also significantly reduced plasma leptin to a much lower degree (Fig. 6*F*). The OGTT and ITT indicated that Z-551 had similar effects (Fig. 6, *G–I*) to those in WT mice on the HFD (Fig. 2, *O–Q*) by ameliorating the glucose intolerance and improving the reduced insulin sensitivity induced by the HFD. Additionally, Z-551 significantly reduced fasting plasma glucose and insulin levels to lower degrees (Fig. 6, *G* and *H*). In contrast, Z-551 did not reduce fasting plasma TG and FFA levels (Fig. 6, *J* and *K*), suggesting that PPARα activation by Z-551 administration is necessary for the reduction of fasting plasma TG and FFA levels. Z-551 had no effect on liver weight in PPARα-deficient mice compared with the control

(Fig. 6*L*), whereas Z-551 significantly increased liver weight in WT mice on the HFD (Fig. 2*H*). These results indicate that PPARα activation by Z-551 was likely to cause the liver hypertrophy in mice.

(ii) Effects of PPARγ Antagonist, CZD-2, in WT Mice on the HFD—CZD-2 is a selective PPARγ antagonist with IC_{50} of 844 nM for mouse PPARγ and its antagonistic activity is equivalent to that of Z-551 (Fig. 1). In WT mice on the HFD, CZD-2 exhibited very similar effects with different intensities (Fig. 7, *A–E, I,* and *J*) compared with those of Z-551 in PPARα-deficient mice on the HFD as described above (Fig. 6) except some effects. The OGTT indicated that CZD-2 decreased plasma insulin, without any difference in plasma glucose levels compared with the con-
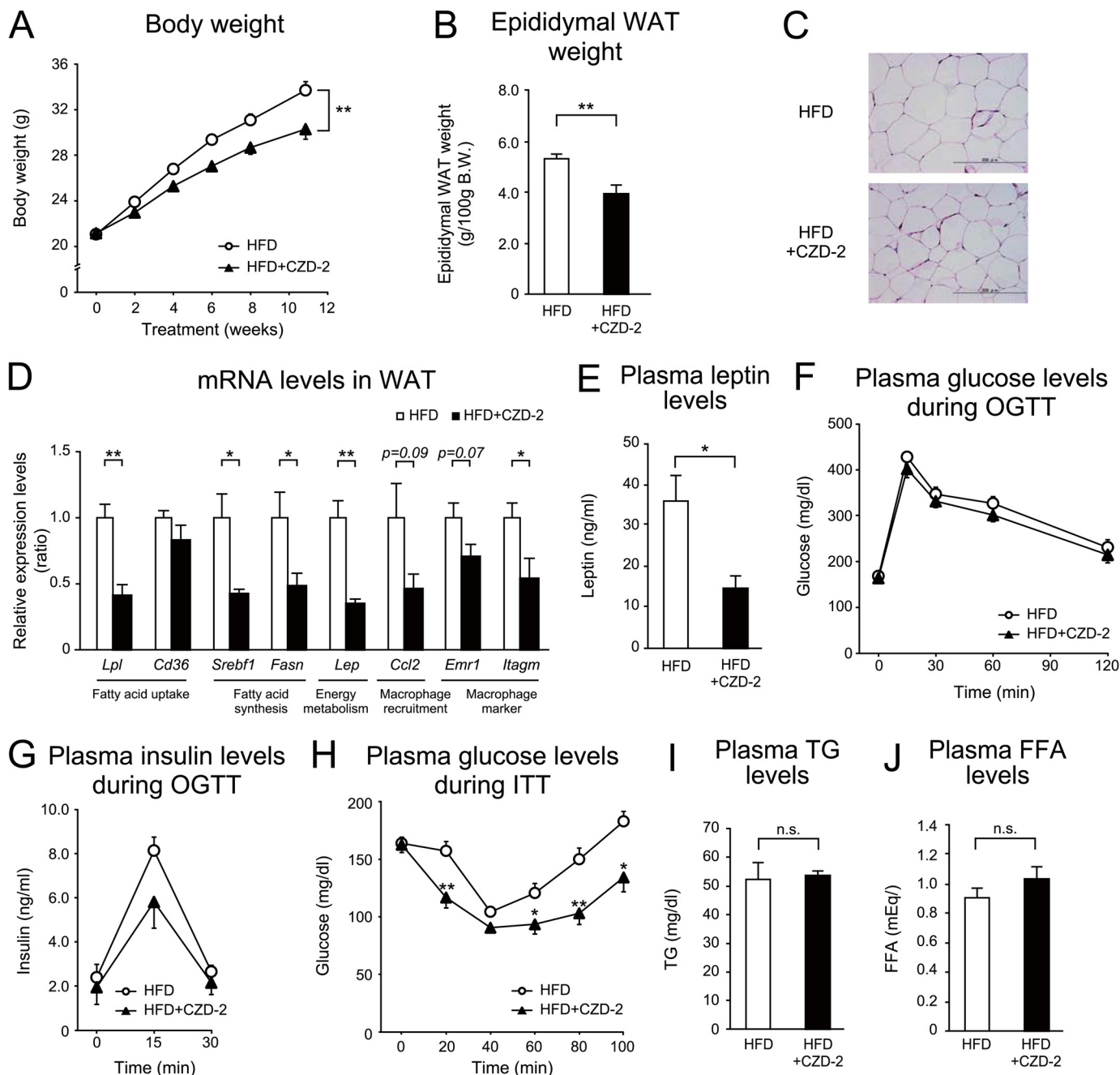
FIGURE 7. **PPARγ antagonist, CZD-2, indicates a part of the preventive effects of Z-551 on diet-induced obesity and metabolic disorders in WT mice.** 4-week-old male WT mice were acclimated to the HFD for 1 week followed by administration of CZD-2 for 11 weeks. *A* and *B*, changes in body weight (*A*), and epididymal WAT weight (*B*) in WT mice on the HFD (*white*) or HFD+CZD-2 (*black*). *C*, morphology of epididymal WAT. Scale bars indicate 200 μm. *D*, mRNA expression levels in epididymal WAT. *E*, plasma leptin Week 11 after CZD-2 administration. *F* and *G*, plasma glucose (*F*) and insulin (*G*) in the OGTT Week 10 after CZD-2 administration. *H*, plasma glucose in the ITT Week 9 after CZD-2 administration. In the OGTT, glucose (1.5 g/kg BW) was orally administered after 6-h fasting. In the ITT, insulin (0.75 unit/kg BW) was intraperitoneally injected. Blood samples were obtained at the indicated times. *I* and *J*, plasma TG (*I*) and FFA (*J*) Week 10 after CZD-2 administration. All results are expressed as mean ± S.E. (n = 6). *, $p < 0.05$; **, $p < 0.01$; *n.s.*, not significant.

trol (Fig. 7, *F* and *G*). The ITT indicated that CZD-2 had a significant decrease in plasma glucose levels after insulin injection (Fig. 7*H*), suggesting that a selective PPARγ antagonist significantly improves insulin sensitivity.

Taken together, these findings indicate that not only PPARα agonistic activity but also PPARγ antagonistic activity of Z-551 is required for ameliorating HFD-induced obesity, insulin resistance, and abnormal glucose and lipid metabolisms.

Z-551 Has No Effect on Bone Loss in WT Mice on the HFD— pQCT, MRI, and MRS were used to elucidate the effect of Z-551 on bone loss in the femur of WT mice on the HFD. In this experiment, both Z-551 (0.01%, 0.03%, and 0.1%) and rosiglitazone (0.01% and 0.03%) markedly improved hyperglycemia and insulin sensitivity in the mice (data not shown). Rosiglitazone exhibited medulla ossium flava (fatty or yellow marrow), and significantly decreased total and trabecular bone mineral den-
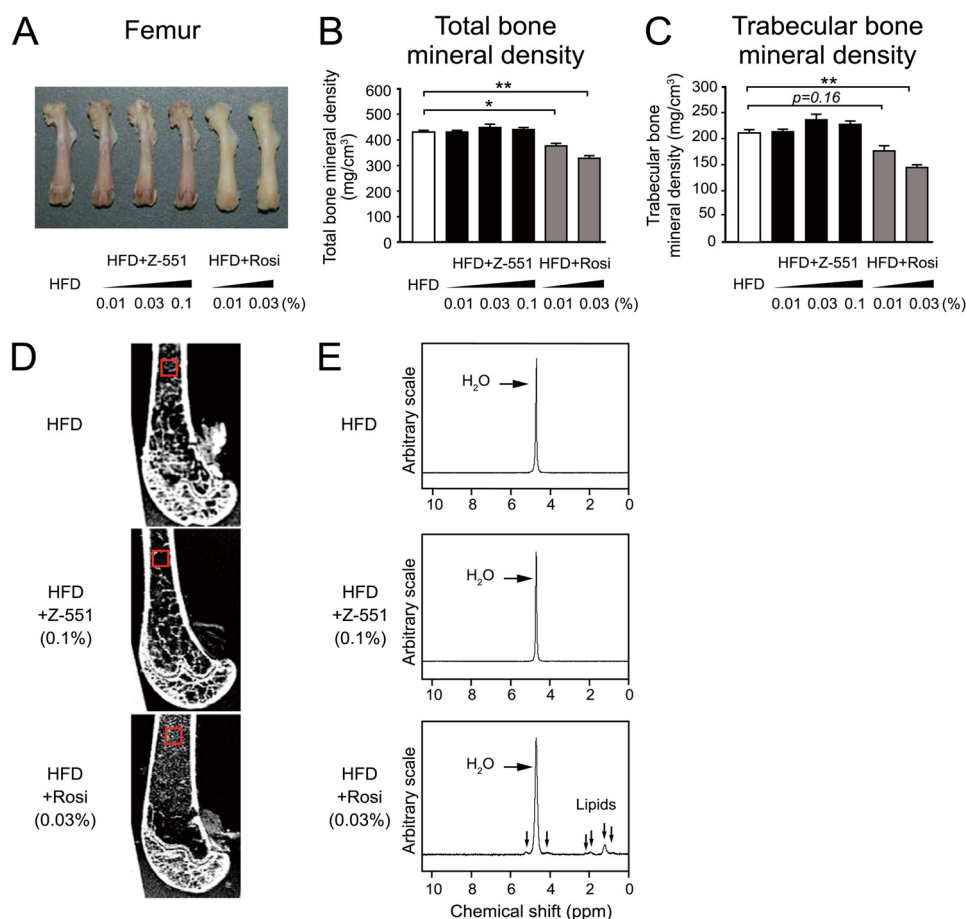
FIGURE 8. **Z-551 shows no effect on bone loss in WT mice.** 4-week-old male WT mice were acclimatized to the HFD for 1 week followed by administration of Z-551 or rosiglitazone for 16 weeks. Z-551 and rosiglitazone were given as a food admixture at 0.01%, 0.03%, or 0.1% (*w/w*). *A*, bone morphology of femur. *B* and *C*, total (*B*) and trabecular (*C*) bone mineral densities of the proximal femur in WT mice on the HFD (*white*), HFD+Z-551 (*black*), or HFD+rosiglitazone (Rosi) (*gray*). Results are expressed as mean ± S.E. ($n = 12$). *D*, MRIs of vertical section of the proximal femur. *E*, 1H-MR spectra obtained from the proximal femur (*red square*). The *downward arrows* in the spectra indicate signals of lipids. *, $p < 0.05$; **, $p < 0.01$.

sities, leading to the trabecular bone loss in the proximal femur of mice (Fig. 8, *A–D*) as previously reported (35). On the other hand, Z-551 had no effect on morphology, color, bone mineral density, and MRI of the proximal femur in the mice compared with the control (Fig. 8, *A–D*). MRS analysis confirms that Z-551 had a closely similar spectrum to that of the control obtained from the proximal femur of mice, whereas rosiglitazone showed new signals of 1H-MRS, indicating the presence of lipids (Fig. 8*E*). These results suggest that Z-551 has no effect on bone loss, whereas rosiglitazone increases the adiposity of bone marrow, leading to an increased risk of bone fracture.

Discussion

In the present study, we investigated the preventive and therapeutic effects of Z-551 using WT mice and WT DIO mice on the HFD to elucidate the mechanisms of Z-551 actions, and thereby examining its potential of being a clinically useful drug for diet-induced obesity and obesity-related metabolic disorders such as insulin resistance, type 2 diabetes, dyslipidemia, and fatty liver diseases.

We demonstrated that Z-551 had anti-obesity effects in both WT mice and WT DIO mice, and unique features of suppressing body weight gain without any reduction of food intake. The gene expression analysis suggests that the anti-obesity effects of

Z-551 are caused by the suppression of increased WAT weight due to the inhibition of fatty acid uptake, and fatty acid synthesis in the adipose tissue, and the activation of fatty acid uptake, fatty acid oxidation, and energy expenditure in the liver. Obesity reportedly causes the onset of leptin resistance with hyperleptinemia and a decline in basal metabolism including thermogenesis (36–38). Leptin is an important adipokine that plays a key role in the regulation of energy intake and expenditure. The present study demonstrates that the anti-obesity effects of Z-551 lead to a significant decrease in plasma leptin levels and the significant elevation in rectal temperature and oxygen consumption during dark phase, suggesting increased energy expenditure. In addition, Z-551 significantly increased the expression levels of BAT markers of thermogenesis. These data raised the possibility that an enhanced BAT thermogenesis could be an underlying cause of the increase in energy expenditure induced by Z-551. Since there are reports to the effect that PPARα agonists increase fatty acid combustion in the liver and promote lipid degradation in the adipose tissue (11, 15), and PPARγ antagonists show anti-obesity effects (24, 25), we consider that both PPARα agonistic and PPARγ antagonistic activities of Z-551 contribute to the anti-obesity effects. In fact, the effects, of Z-551 in PPARα-deficient mice and CZD-2 in
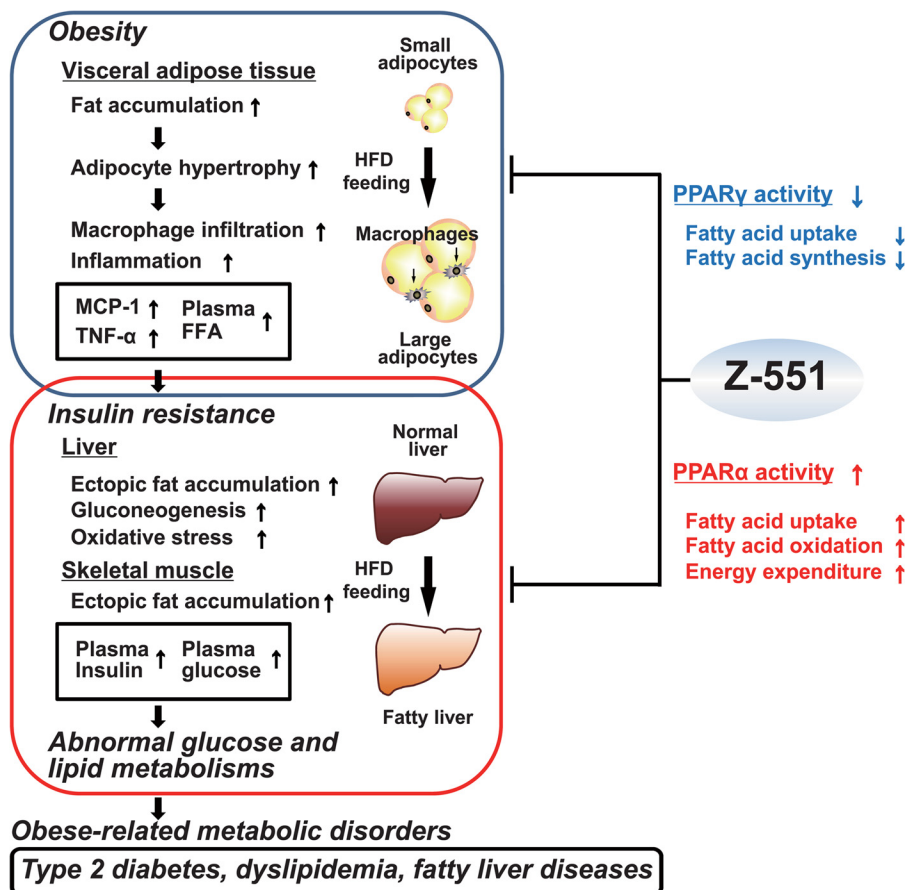
FIGURE 9. **Putative mechanisms of action for Z-551 having both PPARα agonistic and PPARγ antagonistic activities.**

WT mice suggest that the anti-obesity effects of Z-551 are not only due to the PPARα activation but also due to the PPARγ inhibition.

The effects of Z-551 on amelioration of insulin resistance were examined. In WT and WT DIO mice, the OGTT and ITT indicated that Z-551 improved hyperglycemia and hyperinsulinemia induced by the HFD, resulting in amelioration of insulin resistance, whereas the HFD worsened insulin resistance, compared with mice given the ND (data not shown). The observations that treatment with Z-551 markedly reduced plasma insulin levels and blunted the increase in this hormone induced by oral glucose intake in the OGTT (Figs. 2*P* and 4*Q*) may be a consequence of the decreased insulin requirement caused by the improvement in glucose homeostasis and insulin sensitivity induced by Z-551 treatment, since Z-551 does not affect β-cell insulin secretion (data not shown). Z-551 significantly enhanced insulin-stimulated Akt phosphorylation in the liver and skeletal muscle, which is a principal regulatory factor for insulin signaling and glucose metabolism, suggesting that Z-551 improves insulin sensitivity.

It is known that the hypertrophy of visceral adipocytes is closely related to the formation of chronic low-grade inflammation in the periphery and the induction of insulin resistance mediated by abnormal production of pro-inflammatory adipokines (39–41). There are reports to the effect that two types of macrophages, M1 and M2, are found in the adipose tissue suffering from macrophage infiltration, and that increases in M1

macrophages and the M1/M2 polarization of macrophages in the adipose tissue are closely involved in the onset and progression of insulin resistance (42–45). Furthermore, Murakami *et al.* reported that the PPARα activation reduces macrophage-derived inflammation in cultured adipocytes by suppressing the expression of *Tnf* through the inhibition of the nuclear factor-κ B (NF-κB) signaling pathway (46). Z-551 inhibited the expressions of the M1 macrophage markers, *Ccl2*, *Tnf*, and *Tlr4* in the adipose tissue of WT DIO mice, without any effect on the expression of the M2 macrophage marker, *Mrc1*; implicating that Z-551 suppresses the increase in M1 macrophage infiltration into the adipose tissue and induction of inflammation. The gene expression analysis in PPARα-deficient mice administered Z-551 and WT mice administered CZD-2 demonstrates that both Z-551 and CZD-2 tended to inhibit gene expressions of macrophage markers. This observation suggests that both drugs probably inhibited HFD-induced macrophage infiltration into the adipose tissue. Taken together, these findings suggest that Z-551 ameliorates obesity-induced insulin resistance in part by the inhibition of macrophage infiltration and inflammation through not only PPARα activation, but also PPARγ inhibition.

We investigated plasma glucose-lowering effect of Z-551. Z-551 significantly reduced fasting plasma glucose levels in WT and WT DIO mice, whereas a selective PPARγ antagonist, CZD-2, did not reduce the levels in WT mice. On the other hand, Z-551 reduced plasma insulin levels in WT, WT DIO, or

PPARα-deficient mice, while CZD-2 reduced the level in WT mice. These results suggest that PPARα activation is mainly associated with the glucose-lowering action of Z-551, although not only PPARα activation, but also PPARγ inhibition are involved in the improvement of insulin sensitivity. No suppressive effect of Z-551 on food intake indicates involvement of the modulations of glucose and lipid metabolisms including fat accumulation, gluconeogenesis, and glucose utilization in the liver or skeletal muscle in the glucose-lowering action of Z-551. In fact, Z-551 decreased the concentration of hepatic TG content and improved insulin sensitivity. This observation was probably attributable to the inhibition of gluconeogenesis in the liver and the increase in glucose utilization in the skeletal muscle. However, the precise mechanisms for the glucose-lowering effect of Z-551 remain to be elucidated.

Z-551 reduced plasma TG and FFA levels in both WT and WT DIO mice, whereas Z-551 and CZD-2 had no effect on those levels in PPARα-deficient and WT mice, indicating that the reductions of plasma TG and FFA levels are caused by PPARα-dependent action of Z-551, which enhances fatty acid combustion in the liver via PPARα activation. The increase in plasma FFA is known to provoke insulin resistance by inhibiting the insulin-signaling pathway in the liver and skeletal muscle as well as TNF-α, and also inducing inflammation in the adipose tissue infiltrated with macrophages (18, 47). Based on these findings, we have thought that the decrease in plasma FFA levels by Z-551 is partially responsible for the improved insulin resistance.

Excessive fat accumulation and increased oxidative stress due to reactive oxygen species in the liver are known to contribute to the onset of insulin resistance and fatty liver (48, 49). Z-551 has the following effects: to significantly enhance the expressions of PPARα target genes involved in fatty acid uptake and oxidation such as *Lpl* and *Acox1* in the liver in WT and WT DIO mice, and to reduce the concentrations of hepatic TG and TBARS in WT DIO mice. According to these results, Z-551 will be clinically useful for the prevention and treatment of fatty liver diseases including nonalcoholic fatty liver diseases (NAFLD) and nonalcoholic steatohepatitis (NASH).

Several reports on thiazolidinediones (TZDs), PPARγ agonists, demonstrate that these compounds inhibited ectopic fat accumulation and inflammation in the peripheral tissues and increased insulin sensitivity by converting hypertrophic adipocytes (large adipocytes) to normal adipocytes (small adipocytes) (17, 18). TZDs are, however, known to develop various adverse effects including increased body weight, fluid retention, and cardiac failure (50, 51). On the other hand, the present study demonstrates that Z-551 and CZD-2 having PPARγ antagonistic activities inhibited body weight gain. Z-551 had no effect on hematocrit level, which is a marker of fluid retention, whereas rosiglitazone, a TZD, significantly decreased hematocrit level (data not shown). In recent years, epidemiological studies have discussed the problem of bone fragility in diabetic patients administered TZDs and a close relationship between PPARγ activation and bone fracture risk (52, 53). Although the effects of PPARγ inhibition on bone fracture have not been sufficiently elucidated, drugs inhibiting PPARγ are considered to be able to avoid an increased risk of bone fracture. In fact,

Z-551 had no effect on bone mineral density, morphology, and adiposity, whereas rosiglitazone significantly decreased bone mineral density and increased adiposity, leading to an increased risk of bone fracture in the femur of WT mice on the HFD (Fig. 8). Thus, the adverse effects of PPARγ agonists such as TZDs may be avoidable with Z-551.

Analysis of liver weight in WT, WT DIO, and PPARα-deficient mice administered Z-551 shows that the liver hypertrophy caused by Z-551 was likely to be mediated by PPARα activation. However, Z-551 did not significantly increase plasma ALT and AST levels of the liver toxicity markers in WT mice on the HFD (data not shown). We have thought that the risk of liver hypertrophy in humans is low, because PPARα agonists such as fenofibrate used in humans provoke no liver hypertrophy. Chronic hepatic PPARα activation is reported to cause an increased risk of hepatic cancer in rodents, but recent studies have confirmed that there are differences between rodents and humans in the transcription control mechanism of cancer-related genes and gene expression levels of PPARα; thus, the risk of hepatic cancer induced by PPARα activation in humans can be little (54, 55). Based on these findings, Z-551 may have little risk of liver hypertrophy and hepatic cancer in humans. Further studies on the adverse effects of Z-551 are warranted.

The present study demonstrates that a novel and promising PPAR modulator, Z-551, having both PPARα agonistic and PPARγ antagonistic activities, ameliorates HFD-induced obesity, insulin resistance, and impairment of glucose and lipid metabolisms in mice as expected in our concept of drug discovery (Fig. 9). Furthermore, Z-551 causes no adverse effect on body weight gain, and might reduce risks of fluid retention and bone fracture, which are induced by PPARγ agonists including TZDs. In conclusion, we consider that Z-551 will be clinically useful for the prevention or treatment of diet-induced obesity and obesity-related metabolic disorders such as insulin resistance, type 2 diabetes, dyslipidemia, and fatty liver diseases.

References

1. Flegal, K. M., Carroll, M. D., Ogden, C. L., and Curtin, L. R. (2010) Prevalence and trends in obesity among US adults, 1999–2008. *JAMA* **303**, 235–241
2. Kopelman, P. G. (2000) Obesity as a medical problem. *Nature* **404**, 635–643
3. Ahima, R. S. (2006) Adipose tissue as an endocrine organ. *Obesity* **14**, 242S–249S
4. Hotamisligil, G. S., Arner, P., Caro, J. F., Atkinson, R. L., and Spiegelman, B. M. (1995) Increased adipose tissue expression of tumor necrosis factor-α in human obesity and insulin resistance. *J. Clin. Invest.* **95**, 2409–2415
5. Weisberg, S. P., McCann, D., Desai, M., Rosenbaum, M., Leibel, R. L., and

Ferrante, A. W. Jr. (2003) Obesity is associated with macrophage accumulation in adipose tissue. *J. Clin. Invest.* **112,** 1796–1808

6. Xu, H., Barnes, G. T., Yang, Q., Tan, G., Yang, D., Chou, C. J., Sole, J., Nichols, A., Ross, J. S., Tartaglia, L. A., and Chen, H. (2003) Chronic inflammation in fat plays a crucial role in the development of obesity-related insulin resistance. *J. Clin. Invest.* **112,** 1821–1830

7. Desvergne, B., and Wahli, W. (1999) Peroxisome proliferator-activated receptors: nuclear control of metabolism. *Endocr. Rev.* **20,** 649–688

8. Evans, R. M., Barish, G. D., and Wang, Y. X. (2004) PPARs and the complex journey to obesity. *Nat. Med.* **10,** 355–361

9. Lefebvre, P., Chinetti, G., Fruchart, J. C., and Staels, B. (2006) Sorting out the roles of PPARα in energy metabolism and vascular homeostasis. *J. Clin. Invest.* **116,** 571–580

10. Aoyama, T., Peters, J. M., Iritani, N., Nakajima, T., Furihata, K., Hashimoto, T., and Gonzalez, F. J. (1998) Altered constitutive expression of fatty acid-metabolizing enzymes in mice lacking the peroxisome proliferator-activated receptor α (PPARα). *J. Biol. Chem.* **273,** 5678–5684

11. Tsuchida, A., Yamauchi, T., Takekawa, S., Hada, Y., Ito, Y., Maki, T., and Kadowaki, T. (2005) Peroxisome proliferator-activated receptor (PPAR)α activation increases adiponectin receptors and reduces obesity-related inflammation in adipose tissue: comparison of activation of PPARα, PPARγ, and their combination. *Diabetes* **54,** 3358–3370

12. Guerre-Millo, M., Gervois, P., Raspé, E., Madsen, L., Poulain, P., Derudas, B., Herbert, J. M., Winegar, D. A., Willson, T. M., Fruchart, J. C., Berge, R. K., and Staels, B. (2000) Peroxisome proliferator-activated receptor α activators improve insulin sensitivity and reduce adiposity. *J. Biol. Chem.* **275,** 16638–16642

13. Minnich, A., Tian, N., Byan, L., and Bilder, G. (2001) A potent PPARα agonist stimulates mitochondrial fatty acid β-oxidation in liver and skeletal muscle. *Am. J. Physiol. Endocrinol. Metab.* **280,** E270–E279

14. Haluzík, M. M., and Haluzík, M. (2006) PPAR-α and insulin sensitivity. *Physiol. Res.* **55,** 115–122

15. Jeong, S., and Yoon, M. (2009) Fenofibrate inhibits adipocyte hypertrophy and insulin resistance by activating adipose PPARα in high fat diet-induced obese mice. *Exp. Mol. Med.* **41,** 397–405

16. Tontonoz, P., Hu, E., Graves, R. A., Budavari, A. I., and Spiegelman, B. M. (1994) mPPAR γ2: tissue-specific regulator of an adipocyte enhancer. *Genes Dev.* **8,** 1224–1234

17. Okuno, A., Tamemoto, H., Tobe, K., Ueki, K., Mori, Y., Iwamoto, K., Umesono, K., Akanuma, Y., Fujiwara, T., Horikoshi, H., Yazaki, Y., and Kadowaki, T. (1998) Troglitazone increases the number of small adipocytes without the change of white adipose tissue mass in obese Zucker rats. *J. Clin. Invest.* **101,** 1354–1361

18. Yamauchi, T., Kamon, J., Waki, H., Murakami, K., Motojima, K., Komeda, K., Ide, T., Kubota, N., Terauchi, Y., Tobe, K., Miki, H., Tsuchida, A., Akanuma, Y., Nagai, R., Kimura, S., and Kadowaki, T. (2001) The mechanisms by which both heterozygous peroxisome proliferator-activated receptor γ (PPARγ) deficiency and PPARγ agonist improve insulin resistance. *J. Biol. Chem.* **276,** 41245–41254

19. Kubota, N., Terauchi, Y., Miki, H., Tamemoto, H., Yamauchi, T., Komeda, K., Satoh, S., Nakano, R., Ishii, C., Sugiyama, T., Eto, K., Tsubamoto, Y., Okuno, A., Murakami, K., Sekihara, H., Hasegawa, G., Naito, M., Toyoshima, Y., Tanaka, S., Shiota, K., Kitamura, T., Fujita, T., Ezaki, O., Aizawa, S., Nagai, R., Tobe, K., Kimura, S., and Kadowaki, T. (1999) PPARγ mediates high-fat diet-induced adipocyte hypertrophy and insulin resistance. *Mol. Cell* **4,** 597–609

20. Kadowaki, T. (2000) Insights into insulin resistance and type 2 diabetes from knockout mouse models. *J. Clin. Invest.* **106,** 459–465

21. Deeb, S. S., Fajas, L., Nemoto, M., Pihlajämäki, J., Mykkänen, L., Kuusisto, J., Laakso, M., Fujimoto, W., and Auwerx, J. (1998) A Pro12Ala substitution in PPARγ2 associated with decreased receptor activity, lower body mass index and improved insulin sensitivity. *Nat. Genet.* **20,** 284–287

22. Hara, K., Okada, T., Tobe, K., Yasuda, K., Mori, Y., Kadowaki, H., Hagura, R., Akanuma, Y., Kimura, S., Ito, C., and Kadowaki, T. (2000) The Pro12Ala polymorphism in PPAR γ2 may confer resistance to type 2 diabetes. *Biochem. Biophys. Res. Commun.* **271,** 212–216

23. Yamauchi, T., Waki, H., Kamon, J., Murakami, K., Motojima, K., Komeda, K., Miki, H., Kubota, N., Terauchi, Y., Tsuchida, A., Tsuboyama-Kasaoka, N., Yamauchi, N., Ide, T., Hori, W., Kato, S., Fukayama, M., Akanuma, Y., Ezaki, O., Itai, A., Nagai, R., Kimura, S., Tobe, K., Kagechika, H., Shudo, K., and Kadowaki, T. (2001) Inhibition of RXR and PPARγ ameliorates diet-induced obesity and type 2 diabetes. *J. Clin. Invest.* **108,** 1001–1013

24. Rieusset, J., Touri, F., Michalik, L., Escher, P., Desvergne, B., Niesor, E., and Wahli, W. (2002) A new selective peroxisome proliferator-activated receptor γ antagonist with antiobesity and antidiabetic activity. *Mol. Endocrinol.* **16,** 2628–2644

25. Nakano, R., Kurosaki, E., Yoshida, S., Yokono, M., Shimaya, A., Maruyama, T., and Shibasaki, M. (2006) Antagonism of peroxisome proliferator-activated receptor γ prevents high-fat diet-induced obesity *in vivo*. *Biochem. Pharmacol.* **72,** 42–52

26. Cock, T. A., Houten, S. M., and Auwerx, J. (2004) Peroxisome proliferator-activated receptor-γ: too much of a good thing causes harm. *EMBO Rep.* **5,** 142–147

27. Ikemoto, S., Thompson, K. S., Takahashi, M., Itakura, H., Lane, M. D., and Ezaki, O. (1995) High fat diet-induced hyperglycemia: prevention by low level expression of a glucose transporter (GLUT4) minigene in transgenic mice. *Proc. Natl. Acad. Sci. U.S.A.* **92,** 3096–3099

28. Yamauchi, T., Kamon, J., Waki, H., Terauchi, Y., Kubota, N., Hara, K., Mori, Y., Ide, T., Murakami, K., Tsuboyama-Kasaoka, N., Ezaki, O., Akanuma, Y., Gavrilova, O., Vinson, C., Reitman, M.L., Kagechika, H., Shudo, K., Yoda, M., Nakano, Y., Tobe, K., Nagai, R., Kimura, S., Tomita, M., Froguel, P., and Kadowaki, T. (2001) The fat-derived hormone adiponectin reverses insulin resistance associated with both lipoatrophy and obesity. *Nat. Med.* **7,** 941–946

29. Miyake, K., Ogawa, W., Matsumoto, M., Nakamura, T., Sakaue, H., and Kasuga, M. (2002) Hyperinsulinemia, glucose intolerance, and dyslipidemia induced by acute inhibition of phosphoinositide 3-kinase signaling in the liver. *J. Clin. Invest.* **110,** 1483–1491

30. Iwabu, M., Yamauchi, T., Okada-Iwabu, M., Sato, K., Nakagawa, T., Funata, M., Yamaguchi, M., Namiki, S., Nakayama, R., Tabata, M., Ogata, H., Kubota, N., Takamoto, I., Hayashi, Y. K., Yamauchi, N., Waki, H., Fukayama, M., Nishino, I., Tokuyama, K., Ueki, K., Oike, Y., Ishii, S., Hirose, K., Shimizu, T., Touhara, K., and Kadowaki, T. (2010) Adiponectin and AdipoR1 regulate PGC-1α and mitochondria by Ca^{2+} and AMPK/SIRT1. *Nature* **464,** 1313–1319

31. Nio, Y., Yamauchi, T., Iwabu, M., Okada-Iwabu, M., Funata, M., Yamaguchi, M., Ueki, K., and Kadowaki, T. (2012) Monocyte chemoattractant protein-1 (MCP-1) deficiency enhances alternatively activated M2 macrophages and ameliorates insulin resistance and fatty liver in lipoatrophic diabetic A-ZIP transgenic mice. *Diabetologia* **55,** 3350–3358

32. Watanabe, T., Kubota, N., Ohsugi, M., Kubota, T., Takamoto, I., Iwabu, M., Awazawa, M., Katsuyama, H., Hasegawa, C., Tokuyama, K., Moroi, M., Sugi, K., Yamauchi, T., Noda, T., Nagai, R., Terauchi, Y., Tobe, K., Ueki, K., and Kadowaki, T. (2009) Rimonabant ameliorates insulin resistance via both adiponectin-dependent and adiponectin-independent pathways. *J. Biol. Chem.* **284,** 1803–1812

33. Nonaka, K., and Uchiyama, S. (2011) Assessment of volumetric bone mineral density and geometry for hip with clinical CT device. *Clin. Calcium* **21,** 1003–1009

34. Mori, Y., Murakami, M., Arima, Y., Zhu, D., Terayama, Y., Komai, Y., Nakatsuji, Y., Kamimura, D., and Yoshioka, Y. (2014) Early pathological alterations of lower lumber cords detected by ultra-high field MRI in a mouse multiple sclerosis model. *Int. Immunol.* **26,** 93–101

35. Ali, A. A., Weinstein, R. S., Stewart, S. A., Parfitt, A. M., Manolagas, S. C., and Jilka, R. L. (2005) Rosiglitazone causes bone loss in mice by suppressing osteoblast differentiation and bone formation. *Endocrinology* **146,** 1226–1235

36. Friedman, J. M., and Halaas, J. L. (1998) Leptin and the regulation of body weight in mammals. *Nature* **395,** 763–770

37. Auwerx, J., and Staels, B. (1998) Leptin. *Lancet* **351,** 737–742

38. Spiegelman, B. M., and Flier, J. S. (2001) Obesity and the regulation of energy balance. *Cell* **104,** 531–543

39. Uysal, K. T., Wiesbrock, S. M., Marino, M. W., and Hotamisligil, G. S. (1997) Protection from obesity-induced insulin resistance in mice lacking TNF-α function. *Nature* **389,** 610–614

40. Kamei, N., Tobe, K., Suzuki, R., Ohsugi, M., Watanabe, T., Kubota, N.,

Ohtsuka-Kowatari, N., Kumagai, K., Sakamoto, K., Kobayashi, M., Yamauchi, T., Ueki, K., Oishi, Y., Nishimura, S., Manabe, I., Hashimoto, H., Ohnishi, Y., Ogata, H., Tokuyama, K., Tsunoda, M., Ide, T., Murakami, K., Nagai, R., and Kadowaki, T. (2006) Overexpression of monocyte chemoattractant protein-1 in adipose tissues causes macrophage recruitment and insulin resistance. *J. Biol. Chem.* **281,** 26602–26614

41. Toyoda, T., Kamei, Y., Kato, H., Sugita, S., Takeya, M., Suganami, T., and Ogawa, Y. (2008) Effect of peroxisome proliferator-activated receptor-α ligands in the interaction between adipocytes and macrophages in obese adipose tissue. *Obesity* **16,** 1199–1207

42. Bouhlel, M. A., Derudas, B., Rigamonti, E., Dièvart, R., Brozek, J., Haulon, S., Zawadzki, C., Jude, B., Torpier, G., Marx, N., Staels, B., and Chinetti-Gbaguidi, G. (2007) PPARγ activation primes human monocytes into alternative M2 macrophages with anti-inflammatory properties. *Cell Metab.* **6,** 137–143

43. Lumeng, C. N., Bodzin, J. L., and Saltiel, A. R. (2007) Obesity induces a phenotypic switch in adipose tissue macrophage polarization. *J. Clin. Invest.* **117,** 175–184

44. Fujisaka, S., Usui, I., Bukhari, A., Ikutani, M., Oya, T., Kanatani, Y., Tsuneyama, K., Nagai, Y., Takatsu, K., Urakaze, M., Kobayashi, M., and Tobe, K. (2009) Regulatory mechanisms for adipose tissue M1 and M2 macrophages in diet-induced obese mice. *Diabetes* **58,** 2574–2582

45. Suganami, T., and Ogawa, Y. (2010) Adipose tissue macrophages: their role in adipose tissue remodeling. *J. Leukoc. Biol.* **88,** 33–39

46. Murakami, K., Bujo, H., Unoki, H., and Saito, Y. (2007) Effect of PPARα activation of macrophages on the secretion of inflammatory cytokines in cultured adipocytes. *Eur. J. Pharmacol.* **561,** 206–213

47. Suganami, T., Nishida, J., and Ogawa, Y. (2005) A paracrine loop between adipocytes and macrophages aggravates inflammatory changes: role of free fatty acids and tumor necrosis factor α. *Arterioscler. Thromb. Vasc. Biol.* **25,** 2062–2068

48. Inoue, I., Noji, S., Shen, M. Z., Takahashi, K., and Katayama, S. (1997) The peroxisome proliferator-activated receptor α (PPARα) regulates the plasma thiobarbituric acid-reactive substance (TBARS) level. *Biochem. Biophys. Res. Commun.* **237,** 606–610

49. Furukawa, S., Fujita, T., Shimabukuro, M., Iwaki, M., Yamada, Y., Nakajima, Y., Nakayama, O., Makishima, M., Matsuda, M., and Shimomura, I. (2004) Increased oxidative stress in obesity and its impact on metabolic syndrome. *J. Clin. Invest.* **114,** 1752–1761

50. Lehrke, M., and Lazar, M. A. (2005) The many faces of PPARγ. *Cell* **123,** 993–999

51. Nissen, S. E., and Wolski, K. (2007) Effect of rosiglitazone on the risk of myocardial infarction and death from cardiovascular causes. *N. Engl. J. Med.* **356,** 2457–2471

52. Cariou, B., Charbonnel, B., and Staels, B. (2012) Thiazolidinediones and PPARγ agonists: time for a reassessment. *Trends Endocrinol. Metab.* **23,** 205–215

53. Ahmadian, M., Suh, J. M., Hah, N., Liddle, C., Atkins, A. R., Downes, M., and Evans, R. M. (2013) PPARγ signaling and metabolism: the good, the bad and future. *Nat. Med.* **19,** 557–566

54. Morimura, K., Cheung, C., Ward, J. M., Reddy, J. K., and Gonzalez, F. J. (2006) Differential susceptibility of mice humanized for peroxisome proliferator-activated receptor α to Wy-14,643-induced liver tumorigenesis. *Carcinogenesis* **27,** 1074–1080

55. Gonzalez, F. J., and Shah, Y. M. (2008) PPARα: mechanism of species differences and hepatocarcinogenesis of peroxisome proliferators. *Toxicology* **246,** 2–8